Ionized Bicyclo[2.2.2]oct-2-ene: A Twisted Olefinic Radical Cation Showing Vibronic Coupling

Stephen F. Nelsen,*[a] Laurie A. Reinhardt,[a] Hieu Q. Tran,[a] Timothy Clark,[b] Guo-Fei Chen,[c] Robert S. Pappas,[c] and Ffrancon Williams*[c]

Dedicated to Professor Fabian Gerson

Abstract: The bicyclo[2.2.2]oct-2-ene radical cation ($\mathbf{1}^{\bullet +}$) exhibits matrix ESR spectra that have two very different types of *γ-exo* hydrogens (those hydrogens formally in a W-plan with the alkene π bond), $a(2\,\mathrm{H})$ about 16.9 G and $a(2\,\mathrm{H})$ about 1.9 G, instead of the four equivalent hydrogens as would be the case in an untwisted C_{2v} structure. Moreover, deuterium substitution showed that the vinyl ESR splitting is not resolved (and under about 3.5 G); this is also a result of the twist. Enantiomerization of the C_2 structures is rapid on the ESR timescale above 110 K (barrier estimated at 2.0 kcal mol^{-1}). Density functional theory calculations estimate the twist angle at the double bond to be 11–12 degrees and the barrier as 1.2–2.0 kcal mol^{-1}. Single-configuration restricted Hartree–Fock (RHF) calculations at all levels that were tried give untwisted C_{2v} structures for $\mathbf{1}^{\bullet +}$, while RHF calculations that include configuration interactions (CI) demonstrate that this system undergoes twisting because of a pseudo Jahn–Teller effect (PJTE). Significantly, twisting does not occur until the σ-orbital of the predicted symmetry is included in the CI active space. UHF calculations at all levels that include electron correlation (even semiempirical) predict twisting at the alkene π bond because they allow the filled α and the β hole of the SOMO to have different geometries. The 2,3-dimethylbicyclo[2.2.2]oct-2-ene radical cation ($\mathbf{2}^{\bullet +}$) is twisted significantly less than $\mathbf{1}^{\bullet +}$, but has a similar temperature for maximum line broadening. Neither the 2,3-dioxabicyclo[2.2.2]octane radical cation ($\mathbf{3}^{\bullet +}$) nor its 2,3-dimethyl-2,3-diaza analogue ($\mathbf{5}^{\bullet +}$) shows any evidence of twisting. Calculations show that the orbital energy gap between the SOMO and PJTE-active orbitals for $\mathbf{3}^{\bullet +}$ is too large for significant PJTE stabilization to occur.

Keywords: density functional calculations · EPR spectroscopy · matrix isolation · pseudo Jahn–Teller distortion · radical ions

Introduction

The question of whether the ethylene radical cation adopts a twisted equilibrium structure has been the subject of numerous experimental and theoretical studies over several decades.[1–5] In the gas phase, a twisted form of the ion has been inferred from investigations of the vibrational structure in the Rydberg state,[1] as well as from a careful consideration of the photoelectron spectrum.[2] However, ab initio molecular-orbital calculations have given more ambiguous results, the answer depending largely on the level of the calculation and the choice of basis set.[3, 4] In the most recent theoretical study with highly correlated wave functions,[4] Handy and coworkers calculated only a marginal stabilization energy of about 0.1 kcal mol^{-1} below the planar structure with a twist angle of about 16°; these results deviate substantially from the derived experimental values of 0.67–0.84 kcal mol^{-1} and 25°.[1, 2]

A clear-cut determination of the torsional structure of the ethylene radical cation has also proved to be elusive in the condensed phase.[5] A matrix ESR study of the expected $C_2H_4^{\bullet +}$ formed by radiolytic oxidation in SF_6 and Freons at 4 and 77 K gave poorly resolved signals dominated by the detection of a solvent superhyperfine ^{19}F coupling with only line-broadening effects that could be assigned to weak ^{1}H and ^{13}C hyperfine interactions.[5a] The ^{1}H coupling is indeed expected to become less negative on twisting;[6] this would explain why it is difficult to observe a true signature spectrum

[a] Prof. S. F. Nelsen, Dr. L. A. Reinhardt, H. Q. Tran
Department of Chemistry, University of Wisconsin
1101 University Avenue, Madison, WI 53706-1396 (USA)
Fax: (+1) 608-265-4534

[b] Priv.-Doz. Dr. T. Clark
Technical Director, Computer-Chemie-Centrum
Universität Erlangen-Nürnberg
Nägelbachstrasse 25, 91052 Erlangen (Germany)
Fax: (+49) 9131-852-6565

[c] Prof. F. Williams, G.-F. Chen, Dr. R. S. Pappas
Department of Chemistry, University of Tennessee
1420 Circle Drive, Knoxville, TN 37996-1600 (USA)
Fax: (+1) 865-974-3454
E-mail: ffwilliams@utk.edu

in the solid state. Without a definitive identification of the $C_2H_4^{\bullet+}$ signal carrier, however, the estimated torsional angle of 8–23°, based on the probable magnitude and range of unresolved hyperfine couplings,[5a] can only be regarded as tentative.

In view of these uncertainties regarding the structure of the prototype ethylene radical cation, interest naturally turns to the possible characterization of other twisted olefin radical cations. Cederbaum and co-workers[2] have stressed the importance of vibronic coupling[7] as the basic mechanism for twisting, so that, as a guide to possible examples of this genre, an olefin cation with a small energy gap between ground and excited states is expected a priori to be highly favorable to the process.[7c] However, convincing evidence for a vibronic interaction requires the experimental detection of a double minimum in the potential energy surface,[8a] which, by symmetry, in this case would be along the torsional mode.[8b] We now report ESR and computational studies on the bicyclo[2.2.2]oct-2-ene radical cation, $\mathbf{1}^{\bullet+}$, and its vinyl dimethyl analogue, $\mathbf{2}^{\bullet+}$, that clearly establish that these molecules have such interconverting twisted structures.

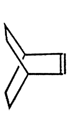
1

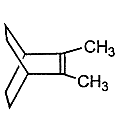

2

Iwasaki and co-workers[9] have previously reported that the ESR spectrum of radiolytically generated $\mathbf{1}^{\bullet+}$ in a $CFCl_2CF_2Cl$ matrix exhibits a 20.4-G 2H triplet at 4.2 K, but a 9.0-G 4H quintet at 106 K. They attributed the low-temperature triplet to splitting by the vinyl hydrogens in an untwisted (C_{2v}) structure having the $C_bC_v{=}C_vC_b$ twist angle $\phi = 0°$, and the higher temperature spectrum to a C_2 twisted species having $\phi \neq 0°$, in which the bridgehead (H_b) and vinyl (H_v) hydrogen splittings were similar enough in size not to be resolved. Although increasing ϕ would, as discussed for $C_2H_4^{\bullet+}$, be expected to make $a(H_v)$ less negative[6] and at the same time increase $a(H_b)$, it did not appear reasonable to us that enough twisting could occur to make the bridgehead splitting as large as 9 G. Our reinvestigation of $\mathbf{1}^{\bullet+}$ shows that the observed splittings do not arise from either vinyl or bridgehead hydrogens but from *γ-exo* hydrogens by means of long-range coupling[10] that is, in fact, suitably enhanced by twisting at the olefinic bond.

Results

ESR splitting constants of $\mathbf{1}^{\bullet+}$ and related species: We also observed a broadened triplet (separation ≅19 G) at low temperature, and a sharper quintet (separation ≅9.4 G) at higher temperature for $\mathbf{1}^{\bullet+}$ in $CFCl_2CF_2Cl$ as well as other matrices. However, the low- and high-temperature spectra are interconverted reversibly as the temperature is cycled over the rather narrow temperature range of 94 to 110 K, and exhibit the alternating line-width behavior expected for two dynamically interconverting sets of 2H splitting constants. Furthermore, [D$_1$]vinyl-substituted $\mathbf{1}^{\bullet+}$ (**[D$_1$]1**$^{\bullet+}$) and unlabelled $\mathbf{1}^{\bullet+}$ give indistinguishable ESR spectra; this shows conclusively that $a(H_v)$ is not resolved at either high or low temperature, in keeping with the previously mentioned expectation[6] that twisting at the olefinic bond reduces the absolute value of the H_v coupling. The four-hydrogen quintet spectrum observed at higher temperature can only be plausibly assigned to the four *γ-exo* hydrogens (H_x) that form a W-plan arrangement[10] with the spin-bearing 1e-π system (see the highlighted bonds and p orbital axis in Scheme 1).

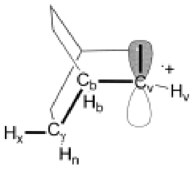

Scheme 1.

The triplet spectrum observed at lower temperature indicates that these four *γ-exo* hydrogens must occur as two pairs that have very different splitting constants in the minimum-energy structure. This is consistent with a significant ϕ twist, contrary to the untwisted structure suggested by Iwasaki and co-workers for the lower-temperature spectrum.[9] The higher-temperature spectrum is then logically interpreted as one that interconverts the two pairs of *γ-exo* hydrogens, the mechanism being ring torsion over a $\phi = 0°$ barrier between equivalent positive and negative ϕ linked to C_2-symmetry energy minima. We will call the two types of *γ-exo* hydrogens in the twisted structure H_{xa} and H_{xn} (for *exo* aligned and *exo* nonaligned, respectively). Scheme 2 shows projections of the C_{2v} and C_2 structures that emphasize how the alignment effect arises.

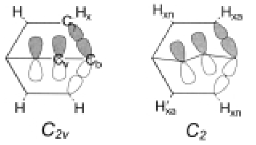

Scheme 2.

For the twisted C=C C_2 species, one pair of C_bC_γ bonds becomes more nearly aligned with the p-orbital axes, while the other pair has a larger angle between the C=C bond and p orbital, and is designated nonaligned. From the 110 K spectrum, the averaged $a(H_x)[4H]$ splitting, $[a(H_{xa}) + a(H_{xn})]/2 = 9.4$ G. Simulations of the spectra, assuming interconverting C_2 twisted structures (Figure 1), give the following information: a) a(H) for the ten hydrogens whose splitting is not resolved in the low-temperature spectrum, that is, $a(H_{xn}[2]$, $a(H_v)[2]$, $a(H_n)[4]$, and $a(H_b)[2]$, are each under about 3.5 G. b) The difference between the γ-exo splittings, $\Delta a(H_x) = a(H_{xa}) - a(H_{xn})$ best fits the observed spectra when $\Delta a(H_x)$ is about 15 G, that is, with $a(H_{xa}) = 16.9$ and $a(H_{xn}) = 1.9$ G. c) Barriers to conformational interconversion of 2.0 kcal mol^{-1} for $\Delta a(H_x) = 15$ G are obtained from the simulations.

The sizes of both $a(H_v)$ and $a(H_x)$ for an undistorted $\mathbf{1}^{\bullet+}$ seemed rather surprising. The vinyl hydrogen splitting for norbornene radical cation is (−)10.6 G[11] and those for cyclopentene, cyclohexene, and *cis*-but-2-ene radical cations lie between (−)8.6 and (−)9.5 G.[12] The average $a(H_x)$ for $\mathbf{1}^{\bullet+}$ is twice that of peroxide $\mathbf{3}^{\bullet+}$, $a(4H_x) = 4.7$ G,[13a] 2.4 times that of the tetracyclic alkene analogue $\mathbf{4}^{\bullet+}$, $a(8H_x) = 3.9$ G,[13b] and 3.8 times that for the analogous dimethylhydrazine radical cation, $\mathbf{5}^{\bullet+}$, $a(4H_x) = 2.6$ G.[13c] In contrast to these results for π radicals, a larger $a(4H_x) = 15.5$ G applies for the isoelectronic 2,3-diazabicyclo[2.2.2]oct-2-ene radical cation, $\mathbf{6}^{\bullet+}$, which is known to be a σ radical at the nitrogens.[14] This is nicely

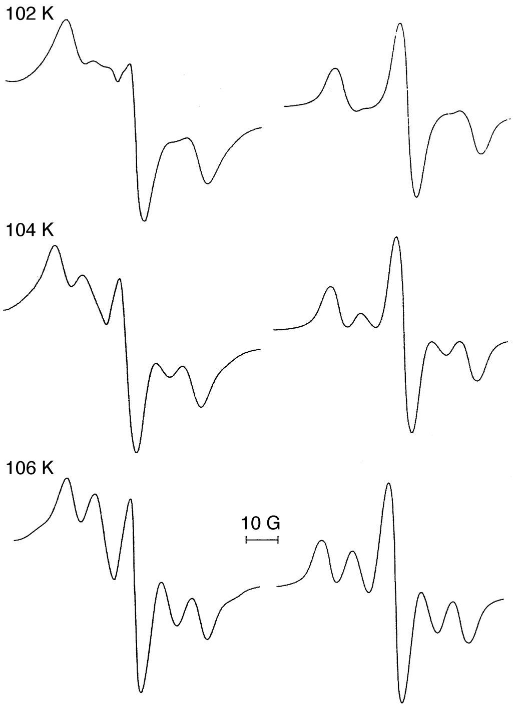

Figure 1. Comparison of observed and simulated spectra for vinyl deuterated $\mathbf{1}^{\cdot+}$ in a $CFCl_2CF_2Cl$ matrix at 102, 104, and 106 K. The simulations used dynamically interconverting pairs of hydrogens with splittings of 16.9 and 1.9 G, as well as $a(2\,H) = 2.4$ G, $a(4\,H) = 1.0$ G, and a Lorentzian line width of 2.1 G, with k_{ex} values of 0.78, 1.16, and $1.58 \times 10^8\,s^{-1}$ at 102, 104, and 106 K respectively.

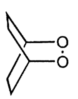

3

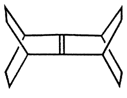

4

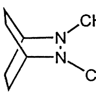

5

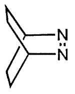

6

consistent with the present findings for $\mathbf{1}^{\cdot+}$, since the introduction of appreciable σ character into the π orbital of $\mathbf{1}^{\cdot+}$ should increase the splitting to the *exo*-hydrogens, as observed.

The ESR spectrum of $\mathbf{2}^{\cdot+}$ (Figure 2) shows a large temperature-independent septet, $a(6\,H) = 18.35$ G, for the methyl hydrogens and also exhibits dynamic behavior for smaller splittings, which can be successfully analyzed as two sets of 2H that interconvert rapidly above 110 K. The average of the smaller splittings is 3.6 G (4H) at high temperature, which is only 38% of the averaged $a(H_x)$ splitting of $\mathbf{1}^{\cdot+}$. From simulations we assigned these splittings as $a(2\,H_{xa}) = 7.0$ G, $a(2\,H_{xn}) = 0.2$ G, so $\Delta a(H_x)$ for $\mathbf{2}^{\cdot+}$ is about 6.8 G or 45% that of $\mathbf{1}^{\cdot+}$. This appears to only be consistent with a significantly smaller ϕ value for $\mathbf{2}^{\cdot+}$ than for $\mathbf{1}^{\cdot+}$. Rather surprisingly, the temperatures of maximum broadening for interconversion of H_{xa} and H_{xn} are rather similar to those for $\mathbf{1}^{\cdot+}$ and $\mathbf{2}^{\cdot+}$. It thus appears from its smaller $a(H_x)$ average and difference that $\mathbf{2}^{\cdot+}$ is significantly less twisted than $\mathbf{1}^{\cdot+}$ but that the barrier to H_x interconversion is not significantly lower. In contrast to $\mathbf{1}^{\cdot+}$ and $\mathbf{2}^{\cdot+}$, no dynamic ESR broadening was observed for peroxide $\mathbf{3}^{\cdot+}$ or hydrazine $\mathbf{5}^{\cdot+}$ in matrices. Therefore, these species either have C_{2v} symmetry or show a significantly smaller sensitivity of $a(H_x)$ to the twisting of equilibrating C_2 structures.

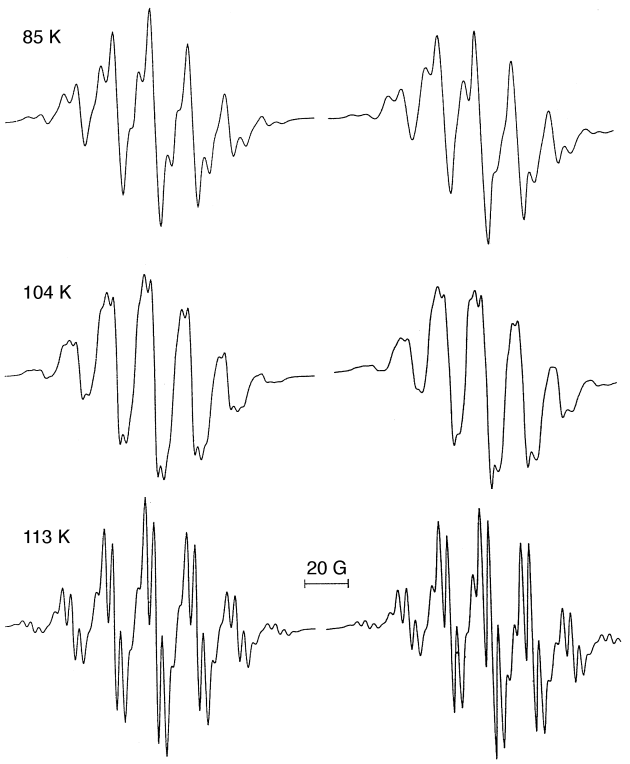

Figure 2. Comparison of observed and simulated spectra for $\mathbf{2}^{\cdot+}$ in a $CFCl_2CF_2Cl$ matrix at 113, 104, and 85 K. The simulations employed $a(6\,H) = 18.35$ G, $a(4\,H) = 0.85$ G, and a pair of dynamically interconverting hydrogens, $a(2\,H) = 7.0$ G, $a(2\,H) = 0.2$ G. Lorentzian line widths and rate constants employed were 1.6 G, $k_{ex} = 8.8 \times 10^8\,s^{-1}$ (113 K, indistinguishable from the fast exchange limit); 2.6 G, $k_{ex} = 1.23 \times 10^8\,s^{-1}$ (104 K); and 3.0 G, $k_{ex} = 4.4 \times 10^7\,s^{-1}$ (85 K).

Pseudo-Jahn–Teller effects considering RHF calculations: The small $a(H_v)$, large $\Delta a(H_x)$, and about 2 kcal mol^{-1} barrier to interconversion of H_{xa} and H_{xn} of $\mathbf{1}^{\cdot+}$ necessitate a significant ϕ value for this molecule. All restricted Hartree–Fock (RHF) calculations that were tried, namely AM1 semiempirical, ROHF/6–31G* (which does not include electron correlation), ROMP2/6–31G* (which includes second-order Møller–Plesset electron correlation), and ROBLYP/6–31G* density functional calculations, incorrectly produce untwisted C_{2v} structures for $\mathbf{1}^{\cdot+}$. Thus, even when electron correlation is included, single configuration RHF calculations are inadequate to describe the proper geometry of this radical cation.

Multiple configuration RHF calculations do allow the observed twisting to be calculated, and we suggest that $\mathbf{1}^{\cdot+}$ provides an exceptionally clear example of the pseudo-Jahn–Teller effect,[7] which we will abbreviate as PJTE. PJTE refers to effects caused by vibronic mixing of a ground electronic configuration with higher energy configurations, such that a geometry of lower symmetry becomes more stable than that of the highest possible symmetry. The gap between the π SOMO ground state of C_{2v} $\mathbf{1}^{\cdot+}$, which has $^2B_1$ symmetry in the coordinate system we used [x direction: center of molecule to bisector of the C=C bond; y: axis of the bridgehead carbons; z: p orbital direction[15]], and the higher-lying σ excited states, including the $^2B_2$ state, can be estimated at ~1.0 eV from the photoelectron spectroscopy data of Bischof and co-workers.[16a] A vibration of the proper symmetry to allow mixing of the states must be present for PJTE mixing to lower the energy.[7] For $\mathbf{1}^{\cdot+}$, an a_2 torsional mode allows such mixing, lowering the symmetry to C_2 by causing ϕ to differ from zero and allowing mixing of the $^2B_1$ ground state with the $^2B_2$ σ-ionized excited state. As the simplest computational model, configuration interaction (CI) calculations with semiempirical AM1-RHF calculations[17a] that employ the single + double excitations CI implementation in VAMP,[17b] which uses the equal numbers of occupied and virtual orbitals as the active space, have been carried out; see the summary in Table 1 and the plots of energy versus twisting angle in Figure 3.

Table 1. Comparison of AM1-RHF calculations for $\mathbf{1}^{\cdot+}$ with and without CI.

active space	Optimum ϕ [°]	Barrier [kcal mol^{-1}]
b_1[a]	0	0
b_1,1*L*UMO	0	0
a_2,b_1,2*L*	0	0
b_2,a_2,b_1,3*L*	11.5	0.33
a_1,b_2,a_2,b_1,4*L*	11.4	0.27

[a] Restricted calculation with the half-electron model.

The RHF SOMO for $\mathbf{1}^{\cdot+}$ is the b_1 π orbital, and the three highest-lying doubly occupied orbitals in these calculations have a_2 (SOMO-1), b_2 (SOMO-2), and a_1 (SOMO-3) symmetry, respectively. When the active space for the CI calculation includes only b_1, a_2, and the first two LUMOs, the symmetry remains C_{2v} ($\phi = 0°$), and almost no change occurs relative to the single-configuration RHF calculation. When the b_2 orbital is included in the active space, the symmetry is lowered to C_2, the $\phi = 0°$ C_{2v} geometry becomes an energy maximum, and $|\phi|$ for the energy minimum increases to almost that same value as when the a_1 orbital is also included. For the largest calculation done, which included the three highest-lying doubly occupied orbitals and the four lowest unoccupied orbitals (this resulted in 44 configurations), the ground state of the radical has a 1.5% contribution from the configuration having the b_2 orbital singly occupied and the b_1 (π) orbital doubly occupied, and very little mixing (<0.1%) of other configurations.

When the energy gap between the ground state and excited states becomes large, PJTE state-mixing becomes small.[7] Photoelectron spectra of dialkyl olefins with unbranched alkyl groups show that the σ,π energy gaps are considerably larger, and little PJTE would be expected. We explored this point using AM1 calculations for the *cis*-but-2-ene radical cation. The single configuration RHF calculation predicts $\phi = 21.1°$, with enthalpy 0.28 kcal mol^{-1} lower than the $\phi = 0°$ form; this is essentially the same result as that obtained for a 44-configuration calculation ($\phi = 20.5°$, barrier = 0.25 kcal mol^{-1}, π orbital 99.9% of the total ground state MO). No PJTE was found, presumably because of the larger energy gap for the *cis*-but-2-ene cation than for $\mathbf{1}^{\cdot+}$.

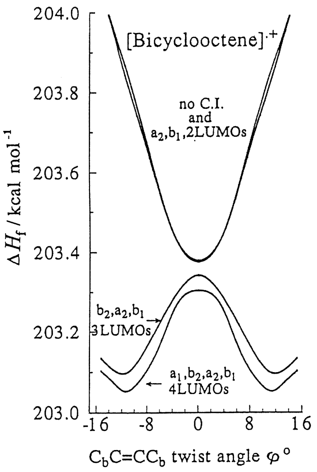

Figure 3. Plots of ΔH_f versus $C_bC{=}CC_b$ twist angle ϕ curves produced by AM1/RHF calculations for $\mathbf{1}^{\cdot+}$ by using CI calculations that have various sizes of active space. When the b_2 σ-orbital that has the right symmetry for PJTE interaction with the π SOMO is included, the system is calculated to change from a C_{2v} single-minimum, untwisted structure to a C_2 double-minimum one.

Peroxide $\mathbf{3}^{\cdot+}$ is nearly isostructural with $\mathbf{1}^{\cdot+}$ (it lacks the vinyl hydrogen atoms) but differs significantly electronically because it has two more electrons in its π system. It does not assume a $\phi \neq 0°$ C_2 structure. Photoelectron spectroscopy indicates that the energy gap between the σ and π orbitals is about 2.0 eV.[16b] As indicated on the left side of Figure 4, because $\mathbf{3}^{\cdot+}$ has a 3e-π bond instead of the 1e-π bond of $\mathbf{1}^{\cdot+}$, its SOMO has a_2 symmetry, and the σ-orbital that has the proper symmetry for PJTE interaction is a_1. This orbital has an energy gap of 4.9 eV from the RHF SOMO for $\mathbf{3}^{\cdot+}$, which is

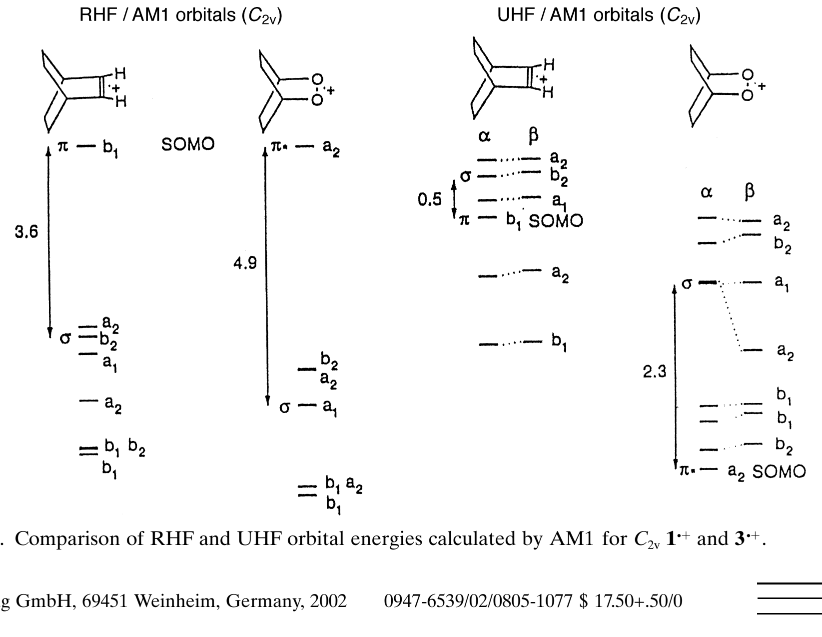

Figure 4. Comparison of RHF and UHF orbital energies calculated by AM1 for C_{2v} $\mathbf{1}^{\cdot+}$ and $\mathbf{3}^{\cdot+}$.

36 % larger than that for $\mathbf{1}^{\bullet+}$. Curiously, the difference is small to cause the qualitatively different results of $\mathbf{1}^{\bullet+}$, which shows an obvious PJTE, and $\mathbf{3}^{\bullet+}$, which does not show the effect. We will return to this point below.

We conclude that twisting in $\mathbf{1}^{\bullet+}$ may be confidently attributed to a PJTE, and that the correct amount of twisting (see below) can be obtained by using CI of RHF calculations that include the σ orbital of proper symmetry to allow the mixing necessary to obtain the twist.

UHF calculations: In contrast to the above single-configuration RHF calculations, unrestricted Hartree–Fock (UHF) calculations that include any electron correlation produce C_2 twisted structures, as summarized in Table 2. As indicated, the UHF/6–31G* calculation, which does not include any electron correlation, still gave a C_{2v} optimized structure. We think it is noteworthy that even the greatly simplified UHF/AM1 method reproduces the torsional twist that requires far more complex and computationally expensive multiconfigurational CI methods when RHF calculations are employed. We also think it is noteworthy that UMP2/6–31G* geometry optimization on this hydrocarbon radical cation apparently does not produce proper twist angles in the bicyclic ring, because the DFT methods make these twist angles considerably different, and also give reasonable predictions of the hyperfine splitting constants (see below), which are quite sensitive to the twist angles.

Table 2. Bicyclic ring twists for UHF calculations on $\mathbf{1}^{\bullet+}$and $\mathbf{2}^{\bullet+}$.

Radical cation	Method	ϕ[a]	ψ[b]	Barrier[c]
$\mathbf{1}^{\bullet+}$	UHF/AM1	– 11.5	– 1.0	0.14
$\mathbf{1}^{\bullet+}$	UHF/6–31G*	0.0	0.0	none
$\mathbf{1}^{\bullet+}$	UMP2/6–31G*	– 8.5	+ 16.7	0.7
$\mathbf{1}^{\bullet+}$	UBLYP/6–31G*	– 12.1	+ 12.5	2.0
$\mathbf{1}^{\bullet+}$	UB3LYP/6–31G*	– 11.0	+ 12.3	1.2
$\mathbf{1}^{\bullet+}$	UB3LYP/6–31 + G*	– 11.3	+ 12.6	1.2
$\mathbf{2}^{\bullet+}$	UB3LYP/6–31 + G*	– 5.7	+ 2.6	0.9

[a] ϕ is the C_bC_v,C_vC_b twist angle; [b] ψ is the C_bCH_2,CH_2C_b twist angle; [c] $\Delta\Delta H$ [kcal mol^{-1}] from the C_{2v} structure.

We suggest that a Weinhold natural-bond-orbital (NBO) analysis[18] clarifies the reason for the single-configuration UHF methods obtaining the twist. The UHF wave function for the C_{2v} structure has the α SOMO in an essentially pure π(C=C) orbital, and the second-order perturbation theory analysis of vicinal interactions that NBO provides gives a 7.12 kcal mol^{-1} interaction of this π SOMO with each of the four equivalent C_b-CH_2 σ_{CC} hybrid orbitals. The α and β π wave functions for the C_2 geometry optimum, for which $\phi = 11.5°$, have significantly different orientations from the σ framework: the π_α SOMO has $\phi_\alpha = 9.7°$, and the unfilled π_β orbital has $\phi_\beta = 13.0°$. The filled π orbital is less twisted (twisting destabilizes π orbitals), while the "hole" is more twisted; this allows larger vicinal interactions with the C_bCH_2 σ_{CC} hybrid orbitals. The second-order perturbation-theory analysis produces 2×11.54 kcal mol^{-1} stabilizations for the aligned σ_{CC} bonds and 2×3.26 kcal mol^{-1} for the nonaligned ones, so there is 1.12 kcal mol^{-1} more stabilization for these interactions than occurs for the C_{2v} structure. The twist leads to a slight decrease of stabilization for several other orbitals, and ΔH_f for the C_2 structure is only 0.14 kcal mol^{-1} lower than that for the C_{2v} structure. According to AM1/UHF calculations then, $\mathbf{1}^{\bullet+}$ undergoes twist to allow improved π-hole, σ_{CC} stabilizing interactions, and it has C_{2v} symmetry by using RHF calculations because the filled and empty π orbitals have been improperly assumed to have the same spatial distribution. In reality, there are of course no two-electron orbitals in an open-shell system, because the odd electron splits the degeneracy of α and β electrons.

Figure 4 compares the RHF/AM1 and UHF/AM1 orbital energies for $\mathbf{1}^{\bullet+}$ and $\mathbf{3}^{\bullet+}$ and shows how different the pictures are. Because electron occupancy has a major effect on orbital stability and this effect is ignored in RHF calculations, the relative energies of the SOMO are extremely different. As frequently occurs for radical cations when using UHF, there are filled σ orbitals higher in energy than the SOMO. It will be noted that the SOMO is far more stabilized when it is centered at oxygen (in $\mathbf{3}^{\bullet+}$) than at carbon (in $\mathbf{1}^{\bullet+}$); this results in a π,σ orbital energy gap for orbitals of the proper symmetry to have undergone PJTE stabilization of 0.5 eV for $\mathbf{1}^{\bullet+}$ and 2.3 eV for $\mathbf{3}^{\bullet+}$. This large difference in orbital energies rationalizes the lack of C_2 structure stabilization for $\mathbf{3}^{\bullet+}$. Figure 4 also emphasizes that the energies of orbitals having different numbers of electrons should not be compared.

Despite the qualitative utility of the very simple AM1 calculations for rationalizing the PJTE in $\mathbf{1}^{\bullet+}$, AM1 calculations have a serious drawback for considering bicyclo[2.2.2]octyl systems quantitatively. They incorrectly get the bicyclic ring torsion at saturated bridges (the $C_bCH_2CH_2C_b$ twist angle ψ, see Scheme 3) to be far too small in bicyclooctanes, as has been thoroughly documented for 2,3-diazabicyclooctanes.[19]

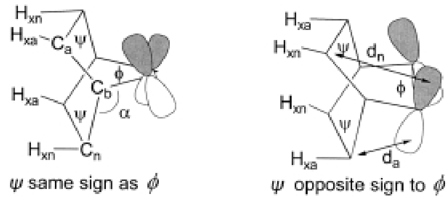

Scheme 3.

Thus, although the UHF/AM1 structure for $\mathbf{1}^{\bullet+}$ has substantial twist at the unsaturated bridge (ϕ), it has these saturated bridges almost untwisted ($\psi = 1.0°$). On steric grounds, one expects the signs of ϕ and ψ to be the same because this leads to the least angle strain; the $C_vC_bC_n$ and $C_vC_bC_a$ angles are the same when the twist angles have the same sign. The small ψ calculated by AM1 is of the same sign as ϕ (see Table 2); however, the minimum energy structures of $\mathbf{1}^{\bullet+}$ calculated by using large basis sets have opposite signs for ϕ and ψ; this makes the $C_vC_bC_a$ angle significantly smaller than the $C_vC_bC_n$ angle. For the B3LYP/6–31G* structure,

0947-6539/02/0805-1078 $ 17.50+.50/0

these angles are 99.9° and 111.6°. As also indicated in Scheme 3, this difference in bond angles makes the distance between a π orbital p-lobe and the aligned C_a carbon smaller than that between the inverse p-lobe and the nonaligned C_n carbon; this is probably important in determining the size of the $a(H_x)$ splittings. The opposite signs for ϕ and ψ presumably arise to allow as much σ-bond,π-hole stabilizing interaction as possible. The lower tendency of alkene radical cations to twist at their $(C{=}C)^+$ bonds as more alkyls are placed on the double bond has been previously pointed out,[6] and is probably responsible for the smaller twist in $\mathbf{2}^{\cdot+}$ than $\mathbf{1}^{\cdot+}$.

It has been established that DFT calculations predict ESR splitting constants rather well for many radicals.[20, 21] Table 3 shows splitting constants calculated for $\mathbf{1}^{\cdot+}$ by using both the pure DFT method UBLYP, and the hybrid DFT/HF method UB3LYP, which are seen to produce rather similar results for both geometry and splitting constants. The principal features of the experimental spectra, a large difference in $a(H_{xa})$ and $a(H_{xn})$, and a small $a(H_v)$, are successfully calculated, although both calculations get a larger value than that observed for $a(H_{xa})$. It should be realized, however, that the splittings calculated for the minimum-energy structure are not those that would be observed experimentally. The $a(H_x)$ and $a(H_v)$ splittings are quite sensitive to both ϕ and ψ twisting, and the energy surface is flat enough that Boltzmann averaging over both ϕ and ψ twisting would have to be considered for accurate estimation of splitting constants.[22] Because both ϕ and ψ must change sign to interconvert C_2 structures, the energy surface is presumably of the "Mexican hat" type that avoids the $\phi = \psi = 0°$ C_{2v} maximum-energy point.[7b,c] The splitting constants predicted for the smaller twists ($\phi = -5.7°$, $\psi = +2.6°$) obtained for $\mathbf{2}^{\cdot+}$ (Table 2): $a(H_{xa}) = 6.15$ (7.0) G, $a(H_{xn}) = -0.06$ (0.2) G, and $a(H_{Me}$, averaged$) = 17.8$ (18.35) G are also seen to be consistent with the observed values given in parentheses.

Table 3. Comparison of DFT calculations (6–31G* basis set) of hyperfine splittings of $\mathbf{1}^{\cdot+}$ with experimental results.

	C_{2v} UBLYP/UB3LYP	C_2(optimized) UBLYP/UB3LYP	Experimental hyperfine splittings[a]
ϕ [°]	$\cong 0$	$-12.1/-11.0$	
ψ [°]	$\cong 0$	$+12.5/+12.3$	
$a(2H_{xa})$,G	$+2.7/+2.6$	$+24.0/+19.3$	16.9
$a(2H_{xn})$,G	$+2.7/+2.6$	$+1.2/-0.7$	1.9
$a(2H_v)$,G	$-11.1/-12.1$	$+0.7/-3.0$	$\ll 3.5$
$a(2H_{na})$[b],G	$-1.2/-1.2$	$+1.0/+0.7$	$\ll 3.5$
$a(2H_{nn})$[b],G	$-1.2/-1.2$	$+0.4/-0.2$	$\ll 3.5$
$a(2H_b)$,G	$-0.6/-0.4$	$-1.0/-0.9$	$\ll 3.5$

[a] Derived from spectral simulations (see Figure 1 and text); [b] H_{na} and H_{nn} refer to aligned and nonaligned *γ-endo* hydrogens, respectively; H_{xa} and H_{xn} are defined according to Scheme 2 and Scheme 3; H_v and H_b refer to vinyl and bridgehead hydrogens, respectively, as indicated in the text.

Discussion

Although the distortion of several organic radical cations has been attributed to vibronic coupling,[23] there are actually very few examples where both the barrier height has been determined and the mixing vibrational mode is well characterized. Most of the previous ESR studies in this area have been concerned with delocalized σ radical cations of alkanes[24] and cycloalkanes,[25] in which matrix annealing effects appear to play a significant role, and the process has been characterized[23–26] as a "matrix-assisted pseudo-Jahn–Teller distortion". The case of the norbornane radical cation[26] is illustrative; this distortion amounts to only a small difference between two pairs of *exo* hydrogens with hyperfine coupling constants of 7.4 and 5.5 G (7.0 and 6.1 G in some instances). Moreover, the four *exo* hydrogens were found to be almost equivalent in some matrices, even at very low temperatures. In other words, the induced distortion, which in this case can take on various forms,[26] is only a very minor perturbation on the expected first-order σ delocalized structure with $a(4H) = 6.5$ G.

Since, in contrast, the norbornene radical cation shows no such delocalization and the "hole" is localized at the olefin bond,[11] an analogous undistorted $\mathbf{1}^{\cdot+}$ would similarly be expected to exhibit about 10-G couplings to the vinyl hydrogens. However, the ESR spectrum of $\mathbf{1}^{\cdot+}$ shows it to be significantly twisted at its 1e-π bond with undetectable vinyl hydrogen splittings. Calculations demonstrate that the saturated bridges are twisted about the same amount in the opposite direction; this results in angle strain, so the distortion clearly has an electronic origin. This is the first case of a bicyclic olefinic system for which the effect of bicyclic torsion upon W-plan γ ESR splittings[10] has been measured, and fortunately they prove to be quite sensitive to torsional angles.

It is interesting to note that the radical cation of bicyclopropylidene has also been shown by ESR studies to assume a twisted geometry at the 1e-π bond,[27] although rapid interconversion between the two twisted forms was not observed in this case. We suggest that vibronic coupling is again the most likely explanation for this twist. The failure to observe the interconversion in this case can probably be attributed to the ease with which the bicyclopropylidene radical cation rearranges to the ring-opened tetramethyleneethane radical cation.[27]

Thus, in comparison with previous ESR studies, it should be stressed that $\mathbf{1}^{\cdot+}$ fulfills several experimental criteria simultaneously for the unequivocal demonstration of vibronic coupling. Firstly, the ESR spectrum is remarkably different in hyperfine structure from that expected for an undistorted form of the radical cation. Secondly, the stability of the radical cation allows it to undergo interconversion between the twisted forms without a competing chemical rearrangement. Finally, the barrier of 2.0 kcal mol^{-1} is such that, whilst it is substantial, it also lies easily within the accessible temperature range of matrix studies. This latter point is important because several small radicals and radical cations that are predicted theoretically to become distorted as a result of vibronic coupling, and which would be amenable to investigation, are unfortunately also characterized by extremely flat potential energy surfaces.[28]

At the same time, RHF-CI calculations also show that $\mathbf{1}^{\cdot+}$ is an excellent example of a molecule that exhibits a significant pseudo-Jahn–Teller (PJTE) effect.[7, 8] UHF methods that include electron correlation allow considerably less expensive geometry optimization for $1^{\cdot+}$ than do RHF calculations because they do not require multiconfigurational calculations to properly estimate the twist at the C=C bond. Density functional theory calculations show that the saturated and unsaturated bridges twist in opposite directions; this must be caused by increased electronic stabilization upon twisting being more important than the bond-angle distortion that opposite twisting requires. Less bicyclic ring torsion occurs for $2^{\cdot+}$ than for $1^{\cdot+}$, but these systems have rather similar barriers to enantiomerization. The lack of C_2 twist in the bicyclic peroxide cation $3^{\cdot+}$ occurs because its different SOMO symmetry and heteroatom substitution causes larger energy gaps to the σ-orbitals that participate in PJTE stabilization upon twisting. It is important, therefore, that in considering PJTE, energy comparisons should be made between orbitals of the same occupancy.

Conclusion

This work has shown that $1^{\cdot+}$ provides an exceptionally clear illustration of the PJTE as it applies to olefin radical cations. The evidence for twisting at the olefin bond comes directly from the fact that since the ESR spectra of $1^{\cdot+}$ and its [D$_1$]vinyl substituted isotopomer **1-d**$^{\cdot+}$ are indistinguishable, there is no measurable hyperfine coupling to the vinyl hydrogens—in remarkable contrast to the spectrum of the nearly isostructural norbornene radical cation[11] and that of other untwisted cycloolefin radical cations,[12] which typically show vinyl couplings of about 10 G. This result nullifies the previous interpretation[9] of the ESR spectrum of $1^{\cdot+}$ in terms of coupling to α (vinyl) and β (bridgehead) hydrogens. Instead, the triplet hyperfine pattern at low temperature is properly interpreted as arising from long-range coupling to the pair of diagonally placed γ-*exo* hydrogens, which are suitably aligned through the W-plan[10] as a result of twisting at the 1e-π bond, which also reduces the vinyl hydrogen coupling.[6] Accordingly, at high temperature, the quintet spectrum with coupling to all four equivalent γ-*exo* hydrogens results from the rapid (on the ESR timescale) interconversion of the two twisted enantiomers by the torsional motion about the olefin bond. In keeping with this dynamic conformational change, the spectral change is reversible. Simulation of these temperature-dependent ESR spectra between 80 and 120 K leads to a calculated barrier of 2.0 kcal mol^{-1} for this enantiomerization. A similar barrier is found for the interconversion of the corresponding enantiomers derived from the 2,3-dimethyl-substituted $1^{\cdot+}$ ($2^{\cdot+}$).

The lowering of symmetry in $1^{\cdot+}$ to the C_2 point group as a result of twisting is attributed to the PJTE brought about through the allowed vibronic coupling of the $^2B_1$ and $^2B_2$ Born–Oppenheimer states in C_{2v} symmetry through the a$_2$ torsional mode. As expected from the basic theory of PJTE,[7] this mixing of the $^2B_1$ π-ionized ground state and the $^2B_2$ σ-ionized excited state is facilitated by the small energy gap of ~1.0 eV between these states, as estimated from photoelectron spectroscopy.[16a] A satisfying corollary is that no indication of twisting is observed[13a] for the isostructural peroxide $3^{\cdot+}$, which has a larger energy gap of ~2.0 eV between the relevant $^2A_2$ π*- and $^2A_1$ σ-states.

Computational studies provide further insight into the role of the PJTE for $1^{\cdot+}$ and reinforce the above conclusions. Thus, whereas the use of single-configuration RHF calculations at all levels predict C_{2v} structures, the inclusion of the σ orbital with b$_2$ symmetry in the CI-active space leads to twisting at the olefin bond. Also, the saturated -CH$_2$CH$_2$- bridges are twisted in the opposite direction; this signifies increased angle strain, so the distortion from C_{2v} symmetry must be electronic in origin. Density functional calculations with both the pure UBYLP and the DFT/HF hybrid UB3LYP methods obtain twisted C_2 structures with barriers in the range of 0.9–2.0 kcal mol^{-1} (Table 2). Moreover, the DFT-calculated hyperfine splittings (Table 3) are in good overall agreement with the experimental values, correctly predicting the large long-range values from the two aligned γ-*exo* hydrogens as well as the small, undetected couplings to the vinyl and bridgehead hydrogens.

Experimental Section

Bicyclo[2.2.2]oct-2-ene (1): This compound was supplied by Aldrich.

Bicyclo[2.2.2]oct-2-ene-2-d (vinyl deuterated **1-d**): Powdered 2,4,6-triisopropylbenzenesulfonyl hydrazide prepared by the method of Reese[29] (3.1 g, 10 mmol) was added to a stirred solution of bicyclo-[2.2.2]oct-2-one (1.3 g, 10 mmol) in methanol (15 mL), and conc. HCl (0.1 mL) was added by syringe. The reaction was stirred for 10 h, cooled, and filtered, and the product was washed with cold methanol. After drying at 0.1 torr for 48 h, 3.23 g (76%) of the sulfonylhydrazone was obtained, decomposed 180–182°, the empirical formula $C_{23}H_{36}N_2O_2S$ was established by high-resolution mass spectrometry. A solution of the sulfonylhydrazone (0.5 g, 1.2 mmol) in ether (7 mL) was stirred at −78 °C, and *tert*-butyllithium (1.53 mL, 1.7 M) in pentane was added dropwise. After being stirred for 30 min, the orange reaction mixture was warmed to 0 °C, and gas (N$_2$) evolved to give a yellow solution, which was then recooled to −78 °C and quenched with D$_2$O (2 mL). The organic layer was collected, dried over MgSO$_4$, and purified by GC to give a colorless oil. ^{1}H NMR (CDCl$_3$) δ = 6.22 (m, 1H), 2.45 (brs, 1.93 H), 1.45 (d, 8H), 1.2 (d, 8H); ^{13}C NMR (CDCl$_3$) δ = 134.4, 134.2 (1:1:1 triplet), 29.9, 29.8, 26.1.

2,3-Dimethylbicyclo[2.2.2]oct-2-ene(2): 2,3-dimethylbicyclo[2.2.2]octan-2-ol (m.p. 86 °C, 21 mg) was heated with a crystal of iodine at 60 °C for 3 h. After the mixture had been cooled, ether was added, and after it had been decolorized with zinc dust, **2** was isolated after drying over MgSO$_4$ and purified by GC.

Dynamic ESR simulations: The program written by Heinzer was employed.[30]

Ab initio calculations: These were carried out at the Computer Center, University of Erlangen, and at the University of Wisconsin by using various versions of the Gaussian program suite.[31]

Radiolytic oxidation: Solutions containing 0.005–0.01 M of **1** and **2** in Freon solvents (CFCl$_3$, CF$_3$CCl$_3$, CF$_2$ClCFCl$_2$) were prepared on a vacuum line in Spectrosil ESR sample tubes (3 mm i.d.) and γ-irradiated at 77 K for a typical radiation dose of 0.2 Mrad (1 Mrad = 10 kGy = 1×10^4 J kg^{-1}). Additional details of sample preparation and reasons for the recommended concentration range are given elsewhere.[10d, 32, 33]

ESR Measurements: After irradiation, the sample tube was quickly transferred from liquid nitrogen into a variable-temperature Dewar insert mounted inside the cavity of an ESR spectrometer (Bruker ER 200D SRC), the initial insert temperature being about 80 K. The X-band microwave frequency was recorded with a Systron-Donner 6054 B counter, and the magnetic fields were determined by an NMR gaussmeter (Bruker ER 035 M). Spectra were recorded at intervals of 5–10 K on progressive annealing, the observed spectral changes being monitored for reversibility by recycling to the lower temperature. The best resolution was obtained with the $CF_2ClCFCl_2$ samples in the range of 85–115 K. In this temperature region, the $CF_2ClCFCl_2$ matrix undergoes a dynamic motion characteristic of "rotator" solids, generating near-isotropic ESR spectra. Moreover, translational diffusion in this matrix is limited below 120 K, thus irreversible bimolecular reactions of radical cations[33] can generally be avoided except in the case of low-molecular-weight solutes. This combination of solid state properties served admirably for monitoring the dynamics of the interconversion between the twisted enantiomeric forms of $\mathbf{1}^{\cdot+}$and $\mathbf{2}^{\cdot+}$, as revealed in Figure 1 and Figure 2 by the characteristic alternating line-width effects.

Acknowledgements

We thank the National Science Foundation for partial financial support of this work under grants CHE-9417946 and CHE-9988727, and the National Science Foundation, National Institutes of Health, the Intel Corporation, and the University of Wisconsin for departmental equipment grants used for the spectrometers and computers (NSF CHE-9522057) employed. The research at the University of Tennessee was supported by the Division of Chemical Sciences, Office of Basic Energy Sciences, Department of Energy, under Grant No. DE-FG02–88ER13852. Special thanks are due to Frank Weinhold for providing a version of AM1 that carries out the NBO analysis and for assistance with Gaussian calculations.

---

[1] a) A. J. Merer, L. Schoonveld, *Can. J. Phys.* **1969**, *47*, 1731; b) R. S. Mulliken, *Tetrahedron* **1959**, *5*, 23; c) P. G. Wilkinson, R. S. Mulliken, *J. Chem. Phys.* **1955**, *23*, 1895; d) R. S. Mulliken, C. C. J. Roothaan, *Chem. Rev.* **1947**, *41*, 219; e) H. Sponer, E. Teller, *Rev. Mod. Phys.* **1941**, *13*, 89; f) W. C. Price, *Phys. Rev.* **1935**, *47*, 444.

[2] a) H. Köppel, W. Domcke, L. S. Cederbaum, W. von Niessen, *J. Chem. Phys.* **1978**, *69*, 4252; b) H. Köppel, W. Domcke, L. S. Cederbaum, S. S. Shaik, *Angew. Chem.* **1983**, *95*, 221; *Angew. Chem. Int. Ed. Engl.* **1983**, *22*, 210.

[3] a) W. A. Lathan, L. A. Curtiss, W. J. Hehre, J. B. Lisle, J. A. Pople, *Progr. Phys. Org. Chem.* **1974**, *11*, 175; b) R. J. Buenker, S. D. Peyerimhoff, H. L. Hsu, *Chem. Phys. Lett.* **1971**, *11*, 65; c) R. Rodwell, M. F. Guest, D. T. Clark, D. Shuttleworth, *Chem. Phys. Lett.* **1977**, *45*, 50; d) A. M. de P. Nicholas, R. J. Boyd, D. R. Arnold, *Can. J. Chem.* **1982**, *60*, 3011.

[4] N. C. Handy, R. H. Nobes, H.-J. Werner, *Chem. Phys. Lett.* **1984**, *110*, 459.

[5] a) K. Toriyama, M. Okazaki, *Appl. Magn. Reson.* **1996**, *11*, 47; b) An earlier study (M. Shiotani, Y. Nagata, J. Sohma, *J. Am. Chem. Soc.* **1984**, *106*, 4640) also claimed to have detected $C_2H_4^{\cdot+}$ in a Freon matrix but in this case a very different ESR spectrum, consisting of five lines with $a(4\,H) \cong 23$ G and observed above 100 K, was assigned to $C_2H_4^{\cdot+}$. However, this signal was subsequently reassigned to a neutral $RCH_2CH_2^{\cdot}$ species, formed by radical addition to C_2H_4 at this higher temperature (J. Fujisawa, S. Sato, K. Shimokoshi, *Chem. Phys. Lett.* **1986**, *124*, 391; see also: X.-Z. Qin, Q.-c. Meng, F. Williams, *J. Am. Chem. Soc.* **1987**, *109*, 6778.

[6] T. Clark, S. F. Nelsen, *J. Am. Chem. Soc.* **1988**, *110*, 868.

[7] a) U. Öpik, M. H. L. Pryce, *Proc. Roy. Soc. A* **1957**, *238*, 425; b) I. B. Bersuker, *The Jahn–Teller Effect and Vibronic Interactions in Modern Chemistry*, Plenum Press, New York, **1984**, p. 61; c) H. Köppel, W. Domcke, L. S. Cederbaum, *Adv. Chem. Phys.* **1984**, *57*, 59.

[8] a) C. J. Ballhausen, *Coord. Chem. Rev.* **1990**, *100*, 29; b) As evidenced in the present work, the experimental detection of a double minimum in the potential energy surface along the mixing a_2 torsional mode constitutes strong evidence that the wave function for $\mathbf{1}^{\cdot+}$ is derived from two Born–Oppenheimer states in C_{2v} symmetry.

[9] K. Nunome, K. Toriyama, M. Iwasaki, *Tetrahedron* **1986**, *42*, 6315.

[10] a) G. A. Russell, *Science*, **1968**, *161*, 423; b) G. A. Russell in *Radical Ions* (Eds.: E. T. Kaiser, L. Kevan), Wiley-Interscience, New York, **1968**, p. 87; c) Y. Ellinger, A. Rassat, R. Subra, G. Berthier, *J. Am. Chem. Soc.* **1973**, *95*, 2372; d) F. W. King, *Chem. Rev.* **1976**, *76*, 157; e) L. D. Snow, F. Williams, *Chem. Phys. Lett.* **1983**, *100*, 198; f) L. D. Snow, F. Williams, *Faraday Discuss. Chem. Soc.* **1984**, *78*, 57–69.

[11] G.-F. Chen, F. Williams, *J. Chem. Soc. Chem. Commun.* **1992**, 670.

[12] a) T. Shida, Y. Egawa, H. Kubodera, T. Kato, *J. Chem. Phys.* **1980**, *23*, 5963; b) J. Fujisawa, S. Sato, K. Shimokoshi, T. Shida, *J. Phys. Chem.* **1985**, *89*, 5487.

[13] a) S. F. Nelsen, M. F. Teasley, A. J. Bloodworth, H. J. Eggelte, *J. Org. Chem.* **1985**, *50*, 3299; b) S. F. Nelsen, D. L. Kapp, *J. Org. Chem.* **1985**, *50*, 1339; c) S. F. Nelsen, R. T. Landis II, *J. Am. Chem. Soc.* **1973**, *95*, 6454.

[14] a) F. Williams, Q.-X. Guo, P. A. Petillo, S. F. Nelsen, *J. Am. Chem. Soc.* **1988**, *110*, 7887; b) F. Gerson, X.-Z. Qin, *Helv. Chim. Acta* **1988**, *71*, 1498.

[15] Since this coordinate system used by the calculation program interchanges the x and z axes from the usual choice for the C_{2v} point group, these axes must be transformed back again with z as the C_2 axis in order to define the B_1 and B_2 symmetry representations used here in accord with the character table.

[16] a) P. Bischof, J. A. Hashmall, E. Heilbronner, V. Hornung, *Helv. Chim. Acta* **1969**, *52*, 1745; b) R. Gleiter, P. Schang, W. Adam, H. J. Eggelte, I. Erden, A. J. Bloodworth, *J. Electron Spectrosc. Relat. Phenom.* **1980**, *19*, 223.

[17] a) AM1 calculations: M. J. S. Dewar, E. G. Zoebisch, E. F. Healy, J. J. P. Stewart, *J. Am. Chem. Soc.* **1985**, *107*, 3902; b) Our AM1 calculations were carried out using various versions of VAMP. T. Clark, A. Alex, B. Beck, J. Chandrasekhar, P. Gedeck, A. Horn, M. Hutter, G. Rauhut, W. Sauer, T. Steinke, VAMP 7.0, OxfordMolecular Ltd., Oxford (UK) **1998**.

[18] A. E. Reed, L. A. Curtiss, F. Weinhold, *Chem. Rev.* **1977**, *88*, 899.

[19] S. F. Nelsen, Y. Wang, D. R. Powell, R. K. Hiyashi, *J. Am. Chem. Soc.* **1993**, *115*, 5246.

[20] a) R. Batra, B. Giese, M. Spichty, G. Gescheidt, K. N. Houk, *J. Phys. Chem.* **1996**, *100*, 18371; b) T. Bally, W. T. Borden, *Rev. Comput. Chem.* **1999**, *13*, 1.

[21] We first understood the ESR spectrum of $\mathbf{1}^{\cdot+}$ from calculations carried out by using a special version of VAMP that predicts splitting constants rather accurately from UHF/AM1 and quartet annihilated UHF/AM1 calculations through use of a neural net. Because these calculations have not been published, we will not consider them here; this system is small enough that carrying out DFT calculations is not a problem.

[22] S. F. Nelsen, T. B. Frigo, Y. Kia. *J. Am. Chem. Soc.* **1989**, *111*, 5387.

[23] K. Toriyama, M. Okazaki, *Acta. Chem. Scand.* **1997**, *51*, 167.

[24] a) K. Toriyama, *Chem. Phys. Lett.* **1991**, *177*, 39; b) K. Toriyama, M. Okazaki, K. Nunome, *J. Chem. Phys.* **1991**, *95*, 3955.

[25] M. Shiotani, M. Lindgren, T. Ichikawa, *J. Am. Chem. Soc.* **1990**, *112*, 967.

[26] M. Okazaki, K. Toriyama, *J. Phys. Chem.* **1993**, *97*, 8212.

[27] F. Gerson, R. Schmidlin, A. de Meijere, T. Spath, *J. Am. Chem. Soc.* **1995**, *117*, 8431.

[28] D. Feller, E. R. Davidson, W. T. Borden, *J. Am. Chem. Soc.* **1983**, *105*, 3347; D. Feller, E. R. Davidson, W. T. Borden, *J. Am. Chem. Soc.* **1984**, *106*, 2513.

[29] N. J. Cusack, L. B. Reese, A. C. Risius, B. Roozpeikar, *Tetrahedron* **1976**, *32*, 2157.

[30] J. Heinzer, *Quantum Chemistry Program Exchange*, No. 209, **1972**.

[31] a) Gaussian 90: M. J. Frisch, M. Head-Gordon, G. W. Trucks, J. B. Foresman, H. B. Schlegel, K. Raghavachari, M. Robb, J. S. Binkley, C. Gonzalez, D. J. Defrees, D. J. Fox, R. A. Whiteside, R. Seeger, C. F. Melius, J. Maker, R. L. Martin, L. R. Kahn, J. J. P. Stewart, S. Topiol, J. A. Pople, Gaussian, Inc., Pittsburgh, PA **1990**; b) *Gaussian 98* (Revision A.7), M. J. Frisch, G. W. Trucks, H. B. Schlegel, G. E. Scuseria, M. A. Robb, J. R. Cheeseman, V. G. Zakrzewski, J. A. Montgomery, R. E. Stratmann, J. C. Burant, S. Dapprich, J. M. Millam, A. D. Daniels, K. N. Kudin, M. C. Strain, O. Farkas, J. Tomasi, V. Barone, M. Cossi, R. Cammi, B. Mennucci, C. Pomelli, C. Adamo, S. Clifford, J. Ochterski, G. A. Petersson, P. Y. Ayala, Q. Cui, K. Morokuma, D. K. Malick, A. D. Rabuck, K. Raghavachari, J. B. Foresman, J. Cioslowski, J. V. Ortiz, B. B. Stefanov, G. Liu, A. Liashenko, P. Piskorz, I. Komaromi, R. Gomperts, R. L. Martin, D. J. Fox, T. Keith, M. A. Al-Laham, C. Y. Peng, A. Nanayakkara, C. Gonzalez, M. Challacombe, P. M. W. Gill, B. G. Johnson, W. Chen, M. W. Wong, J. L. Andres, M. Head-Gordon, E. S. Replogle, J. A. Pople, Gaussian, Inc., Pittsburgh PA, **1998**.

[32] W. Adam, H. Walter, G.-F. Chen, F. Williams, *J. Am. Chem. Soc.* **1992**, *114*, 3007.

[33] F. Williams, X.-Z. Qin, *Radiat. Phys. Chem.* **1988**, *32*, 299.

Received: July 26, 2001 [F3445]